J M M
Journal of Mechanics and MEMS
Special Issue dedicated to Prof. K Y Ye edited by Z M Ye, P Liu and B Sun

ISSN: 0974-8407

9(2) 2017: pp. 357-366

NUMERICAL INVESTIGATION ON NANOINDENTATION RESPONSE OF MULTILAYER THIN FILMS ON A HARD SUBSTRATE

W. G. Jiang[1, 2], C. Yan[2]

ABSTRACT

The nanoindentation behavior of multilayer thin films (MTFSs) with various individual layer thicknesses and different stacking sequence was numerically investigated. The attention was focused on the effects of individual layer thickness and substrate on the load–penetration curve, micro-hardness, and pile-up around the indenter. The numerical simulation showed that the indentation depth required to drive the plastic zone to the interface with the adjacent layer can be considered as a critical depth above which the indentation response is controlled by all constituting layers in a MTFS rather than the top layer. The critical depth and hardness evaluated in a MTFS is sensitive to not only the individual layer thickness but the stacking sequence of the film. In the Cu/Ni/W MTFSs (soft layer on the top), the thinner the individual layer thickness, the smaller the critical penetration depth but the higher the hardness can be observed in the present study. Opposite trend is associated with the W/Ni/Cu MTFSs, i.e., a hard layer on the top. The pile-up ratio around the indenter is proportional to the evolution of plastic zone in the lateral direction.

***Keywords*:** Multilayers; Nano-indentation; Finite element analysis; Substrate effect

1. INTRODUCTION

Multilayer thin film systems (MTFSs) are attracting increasing attention due to potential applications in a broad range of microsystems, such as microelectronic devices and microelectromechanical and nanoelectromechanical systems (MEMS and NEMS) [1~3]. With ever-continuing miniaturization, the individual layers in a MTFS become thinner and thinner and there is a great demand on the mechanical behaviour of the system [4]. The mechanical properties of MTFSs in small volumes have been investigated using nanoindentation [2~3, 5~7]. It was found that MTFSs with a individual layer thickness λ less than 46 nm present higher values of yield stress, Young's modulus, hardness and toughness than those in the single-layer films (CrN and Cr coatings) [7]. Tan and Shen [1] conducted a systematical numerical investigation on the relationship between indentation hardness and overall yield strength of multilayered films. The alternating layers in the films were simplified as laminated composites but the effects of the individual layer thickness and substrate were ignored.

It is well-known that to measure the hardness of a thin film with a substrate, small indentation depth must be used to eliminate the effect of the substrate. The critical indentation depth is only a small fraction of the film thickness. The frequently used one-tenth 'rule of thumb' suggests that the real hardness of a coating can be obtained if the indentation depth is below one tenth the coating thickness [8]. Recently, the applicability of one-tenth rule has been investigated through more rigorous analytical modeling and numerical analysis [9~11]. On the other hand, the substrate effect in MTFSs has not been systematically studied.

On the other hand, because of pile-up and sink-in, the true contact area during indentation can be either underestimated or overestimated by as much as 60% with a rigid conical indenter [12]. Thus, the pile-up and sink-in behavior of single layer films has been investigated by many researchers to quantify the correction factors for

1. School of Materials Science and Engineering, Nanchang Hangkong University, Nanchang 330063, China.
2. School of Engineering Systems, Queensland University of Technology, Brisbane, QLD 4001, Australia.
E-mail: jiangwugui@gmail.com (W.G. Jiang)

hardness measurement [13, 14]. Recently, pile-up behavior in plastically graded materials has been numerically investigated by Choi *et al.* [15]. To the authors' knowledge, little work has been conducted on pile-up and sink-in behavior in MTFSs.

The present study is aimed at analyzing the influences of individual layer thickness on the mechanical and failure behavior of MTFSs. The finite element analysis will be carried out to understand the effects of layer thickness and substrate materials on load-displacement (*P*–*h*) curves, nanohardness and pile-up ratios. The Cu/Ni/W and W/Ni/Cu multilayer thin films were taken as examples because its constituting materials had been understood clearly.

2. FINITE ELEMENT MODELING

Triple-layer (Cu/Ni/W) MTFSs were numerically investigated in the present study. Cu/Ni/W multilayer thin films with a total thickness of 900 nm were placed on 525-µm-thick Si (100) substrates. The thickness of the individual layer (λ) was selected as 30, 60, 100, 150 and 300 nm. Equal individual layer thickness was applied to the Cu, Ni and W layers. The finite element was conducted for the nanoindentation test using a rigid conical indenter with a 160-nm tip radius, as shown in Fig. 1. The included semi-angle of the conical indenter was chosen as 70.3°. For comparison, single layer copper, nickel, tungsten films and MTFSs with a reversed deposition sequence, i.e., W/Ni/Cu were also simulated. The thickness of the films and substrate was the same as the Cu/Ni/W system, i.e., 0.9 and 525 µm, respectively. The simulations were performed using the commercial software ABAQUS 6.7 (SIMULIA, Providence, RI, USA). The thin film and substrate were represented as two infinite solids. Fig. 1 also shows mesh

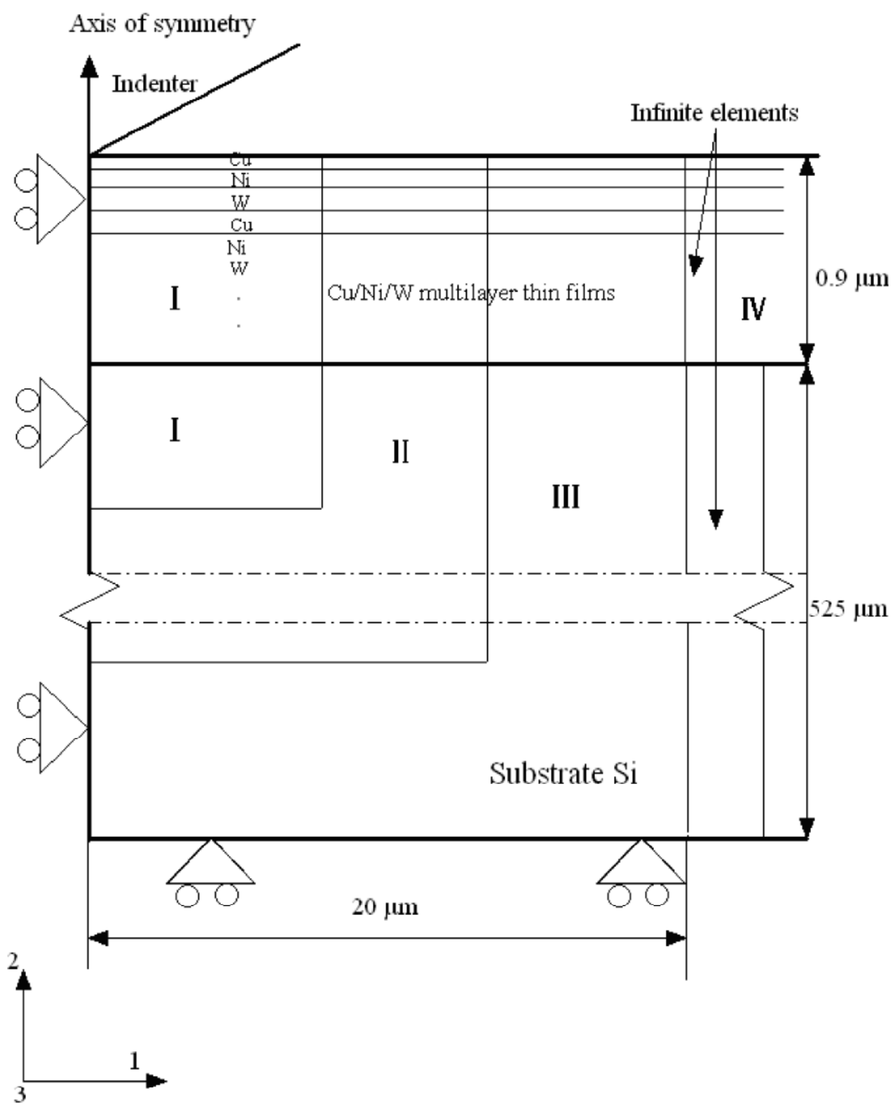

Figure 1: Schematic of the Numerical Model and Boundary Conditions

distribution and the boundary conditions, which is similar to the work of Huang and Pelegri [16]. The smallest rectangular elements (10 nm×20 nm) were allocated in the zone just beneath the indenter (Zone I). The interface between the indenter and the film surface was defined as a finite sliding frictionless surface. All interfaces between adjacent layers were assumed to be perfectly bonded so the displacement field across the interface is continuous.

The Cu, Ni and W were assumed to be elastic-perfectly-plastic solid, using the classical metal plasticity model in ABAQUS [17]. Rate independent plasticity and von Mises yield function were used. The substrate was modeled as an elastic solid. The material parameters used in the simulations are listed in Table 1.

Table 1
Material Properties for the Finite Element Simulation [18~20]

	Copper	*Nickel*	*Tungsten*	*Silicon*
Elastic modulus, *E* (GPa)	145	200	410	163
Poisson's ratio, *v*	0.25	0.312	0.26	0.22
Yield strength (MPa), *Y*	927	1881	3490	
c = Y/E	0.0064	0.0094	0.0085	

3. RESULTS AND DISCUSSION

3.1. P–h curves

The numerical load-penetration (*P–h*) curves of the Cu/Ni/W MTFSs with various individual layer thicknesses are shown in Fig. 2. At the same indentation penetration, the load required increases with decrease of the individual layer thickness, λ.

In general, complex stress state under an indenter is expected even for homogeneous materials. The heterogeneity introduced by the alternating hard and soft layers in MTFSs makes this more complicated [21]. Therefore, detailed finite element analysis is necessary to understand the experimental observation.

Although the indentation is normally conducted under a compression load, significant local tensile stresses along certain directions can still be generated. Fig. 3 shows that the contour plots of the radial and circumferential stress components σ_{radial} and $\sigma_{cricumferential}$ corresponding to the indentation depths of 100 and 300 nm, where the

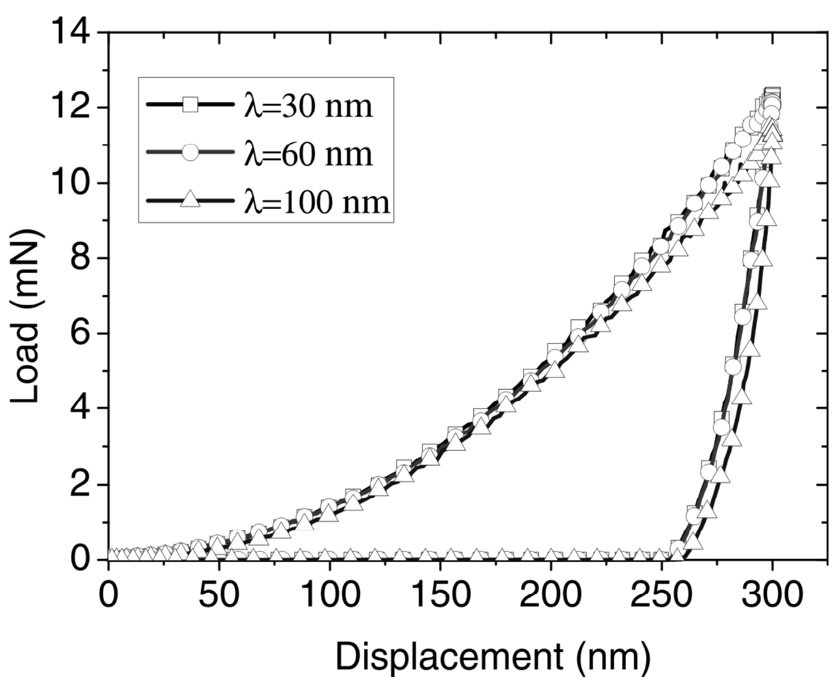

Figure 2: Simulated *P–h* Curves when λ=30, 60 and 100 nm

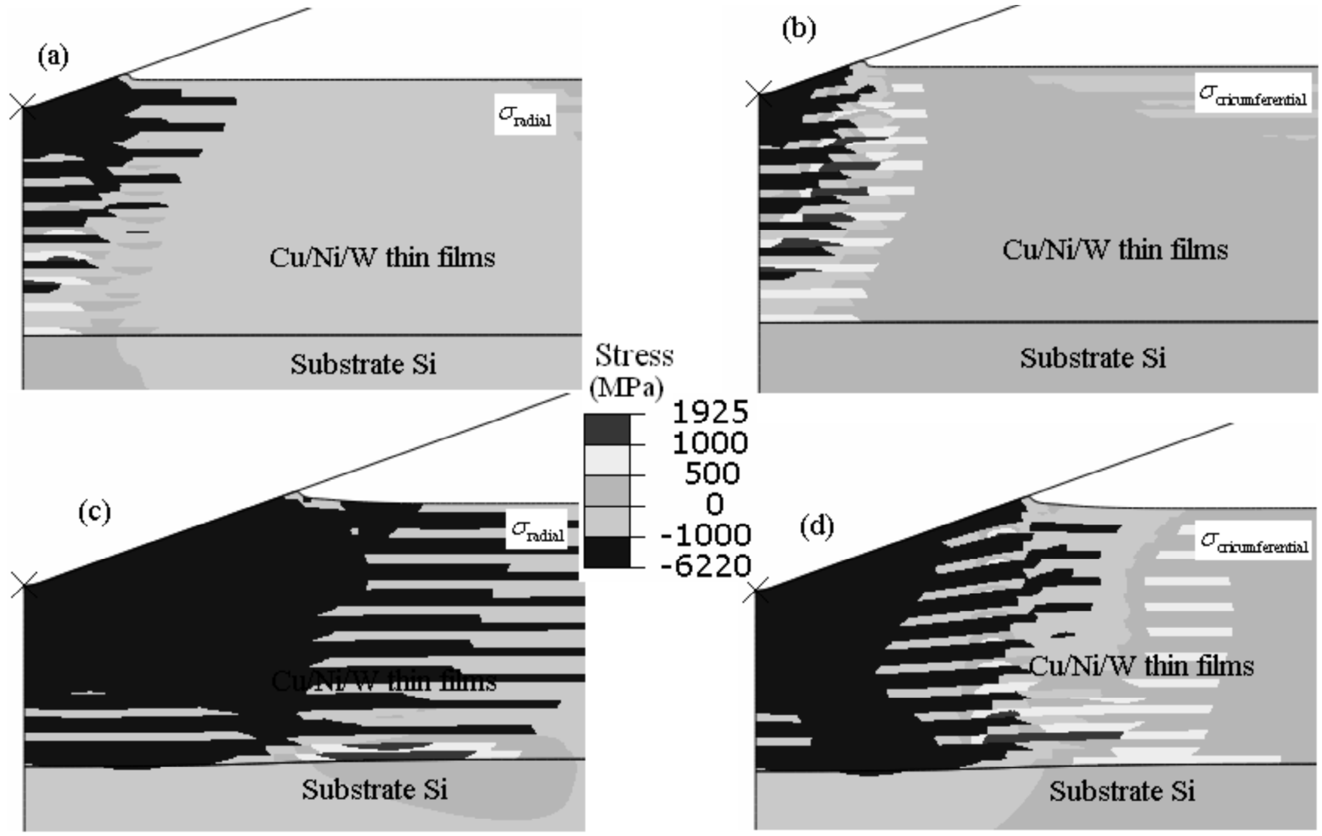

Figure 3: Contours of Stresses under the Indenter for the Films with λ = 30 nm (a) σ_{radial}, Indentation Depth=100 nm, (b) $\sigma_{cricumferential}$, Indentation Depth = 100 nm, (c) σ_{radial}, Indentation Depth = 300 nm and (d) $\sigma_{cricumferential}$, Indentation depth = 300 nm

individual layer thickness λ is 30 nm. The stress distribution is very different in the Cu, Ni and /W layers. When the indentation depth is relatively small, high tensile stress can be seen underneath the indenter and a similar distribution is observed for both the σ_{radial} and $\sigma_{circumferential}$. Moreover, in Figs. 3a and 3b, it can be seen that the area occupied by the tensile circumference stress $\sigma_{circumferential}$ is larger than that of the tensile radial stress σ_{radial}. With increase of indentation depth, as shown in Figs. 3c and 3d, the high tensile stresses move towards the lower layers, which may cause cracks in the brittle tungsten layers.

The finite element simulated *P–h* curves of the single layered Cu and W films, Cu/Ni/W and W/Ni/Cu MTFSs are shown in Fig. 4. As expected, *P–h* curves of the MTFSs are dominated by the top layer when the indentation depth is below a critical value. For the Cu/Ni/W MTFSs, these critical depths are about 30 nm and 70 nm for λ = 100 nm and 300 nm, respectively, as shown in Fig. 4a. Fig. 4b shows that for W/Ni/Cu MTFSs, these critical depths are about 10 nm and 30 nm for λ = 100 nm and 300 nm, respectively. This indicates that the critical penetration depth in a multilayered film, below which the *P–h* curves of the MTFSs are dominated by the top layer, is sensitive to the deposition sequence. When the top layer is a softer material, e.g., Cu/Ni/W in our simulations, the critical depth can reach about 25% of the individual layer thickness, while for a hard top layer, e.g., W/Ni/Cu, it is only about 10% of the individual layer thickness, similar to the traditional one-tenth rule.

Figs. 5 and 6 show the evolution of plastic deformation zone in the Cu/Ni/W and W/Ni/Cu MTFSs with λ = 300 nm at a small penetration depth. It can be seen that plastic deformation starts from the top layer and then propagates vertically and laterally to the interface with the adjacent layer. The indentation depths corresponding to the moment at which the plastic zone is in contact with the interface are 70 nm and 30 nm for the Cu/Ni/W and W/Ni/Cu MTFSs with λ = 300 nm, respectively. These depths are exactly the same with those at which the *P–h* curves in a MTFS start to deviate from that of a single layered film (Fig. 4). Thus, the indentation depth required to drive the plastic zone to the interface with the adjacent layer can be considered as a critical depth above which the indentation response is controlled by all constituting layers in a MTFS rather than the top layer. This is similar to the analysis of Panich and Sun on the substrate effects [8].

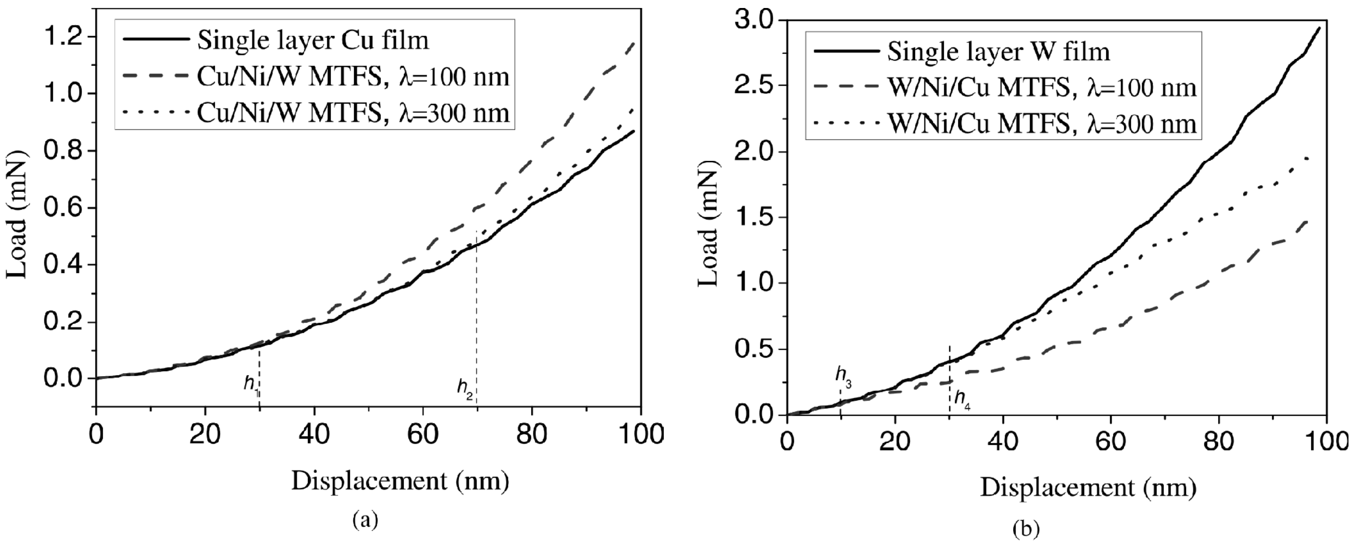

Figure 4: Simulated *P–h* Curves for (a) Single Layer Cu film and Cu/Ni/W MTFSs, and (b) Single Layer W film and W/Ni/Cu MTFSs

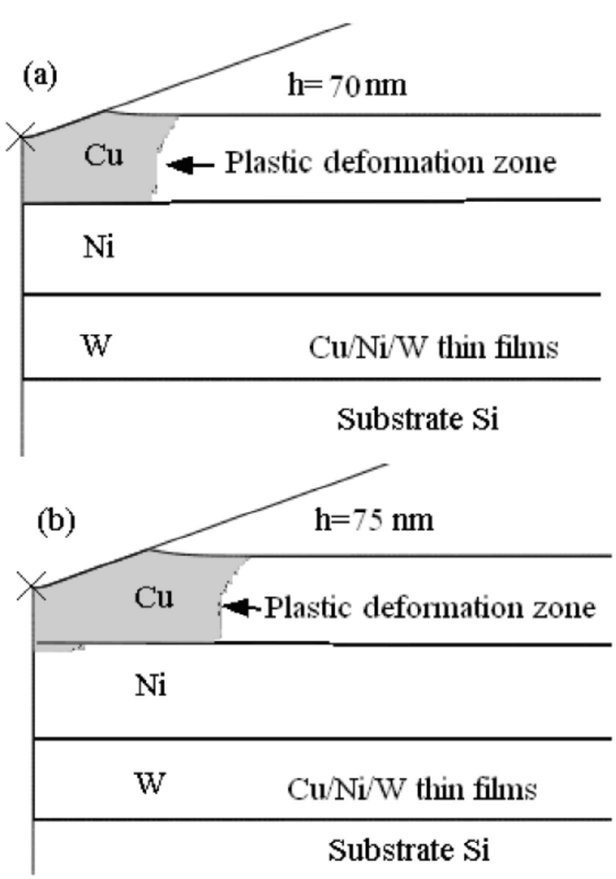

Figure 5: Development of Plastic Deformation Zone in the Cu/Ni/W MTFSs with λ = 300, Corresponding to Different Penetration Depths: (a) 75 nm and (b) 80 nm

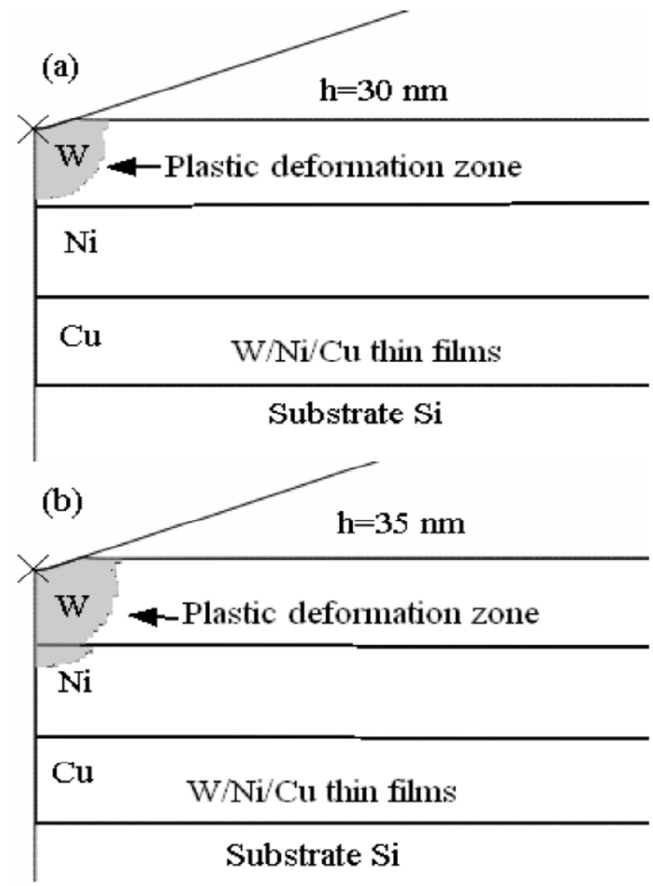

Figure 6: Development of Plastic Deformation Zone in the W/Ni/Cu MTFSs with λ = 300, Corresponding to Different Penetration depths: (a) 30 nm and (b) 35 nm

3.2. Substrate Effect

Figs. 7, 8 and 9 show the interaction between the plastic zone and the substrate in the single layered Cu and W films, Cu/Ni/W and W/Ni/Cu MTFSs with λ = 300 nm corresponding to different indentation depths. With increasing the indentation depth, the plastic zone is in contact with the interface with the adjacent layers and finally with the

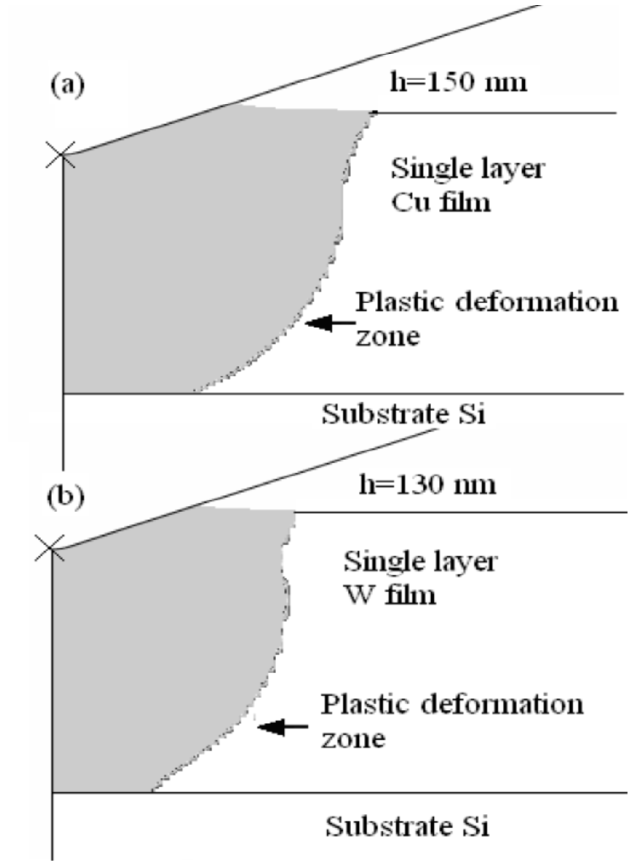

Figure 7: Development of Plastic Deformation Zone Towards the Substrate in Single Layered (a) Cu and (b) W Films

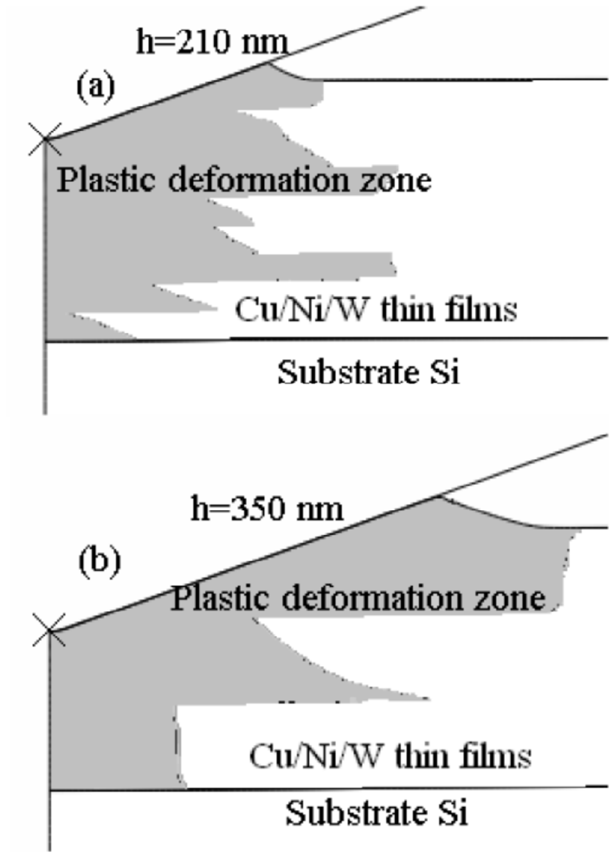

Figure 8: Development of Plastic Deformation Zone towards the Substrate in the Cu/Ni/W MTFSs with λ (a) 100 nm and (b) 300 nm

substrate (Si). If we still define the critical penetration depths as ones at which the plastic zones propagates to the adjacent interfaces, the finite element analysis shows the critical depths are 150 nm and 130 nm for single layered Cu and W films, respectively, which are approximately equal to 15% of the film thicknesses, In Fig. 7, it can be seen that the critical depth for single layered Cu film is higher than that for the W film. We note that the ration of *Y/E* for Cu and W are 0.0064 and 0.0085, respectively. Therefore, it seems a smaller *Y/E* leads to a higher critical depth. This has been observed by other investigators [8].

Unlike the single layered films, the substrate effect in the MTFSs is more complicated. As shown in Fig. 8, the plastic zone propagates to the interface with the Si substrate in the indentation depths of 210 nm (23% of the overall film thickness) and 350 nm (39% of the overall film thickness) for the Cu/Ni/W MTFSs with λ = 100 nm and 300 nm, respectively. In Fig. 9, it is clear that the Si substrate effect can be neglected when the indentation depth is below 150 nm (17% of the film thickness) and 100 nm (11% of the film thickness) for the W/Ni/Cu MTFSs with λ = 100 nm and 300 nm, respectively. Therefore, for the Cu/Ni/W MTFSs, the thinner the individual layer thickness, the smaller the critical penetration depth, whereas for W/Ni/Cu MTFSs, the thinner the individual layer thickness, the higher the critical penetration depth.

3.3. Hardness

To investigate the influence of individual layer thickness on the nanoindentation response, the hardness values and their dependence with indentation depth in the Cu/Ni/W and W/Ni/Cu MTFSs with various λ (30, 100 and 300 nm) were numerically investigated and the results are shown in Fig. 10. The hardness valve is obtained by dividing the contact area from the load directly in the simulated results without considering the Si substrate effect. For comparison, the hardness values for single layered Cu and W films are also presented. For the MTFSs with different stacking sequences, like Cu/Ni/W and W/Ni/Cu, the hardness evaluated are quite different although a same individual layer thickness is used. For a small indentation depth, the hardness is dominated by the top layer and therefore a lower hardness is associated with the Cu/Ni/W film. With increasing the indentation depth, the difference between the hardness evaluated in these two MTFSs is diminished and these curves tend to merge each other. In principle, an identical hardness is expected when the indentation depth is large enough. Within the limited indentation depth used in our simulations, the thinner the individual layer thickness, the higher the hardness for the Cu/Ni/W MTFSs but opposite trend is observed in the W/Ni/Cu MTFSs (Fig. 10).

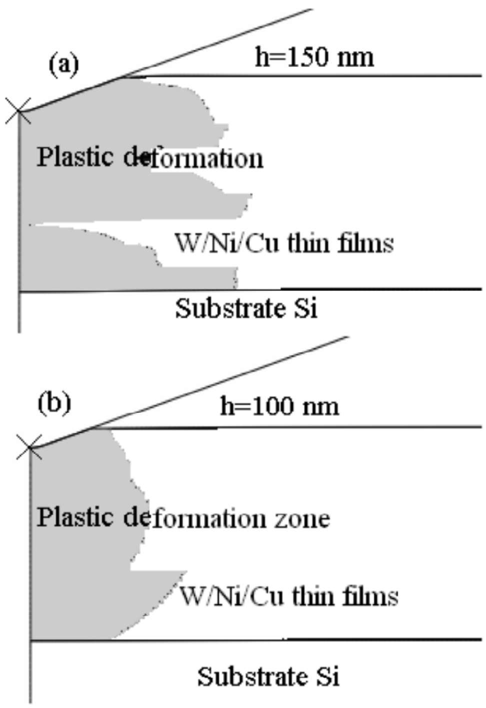

Figure 9: Development of Plastic Deformation Zone Towards the Substrate in the W/Ni/Cu MTFSs with λ (a) 100 nm and (b) 300 nm

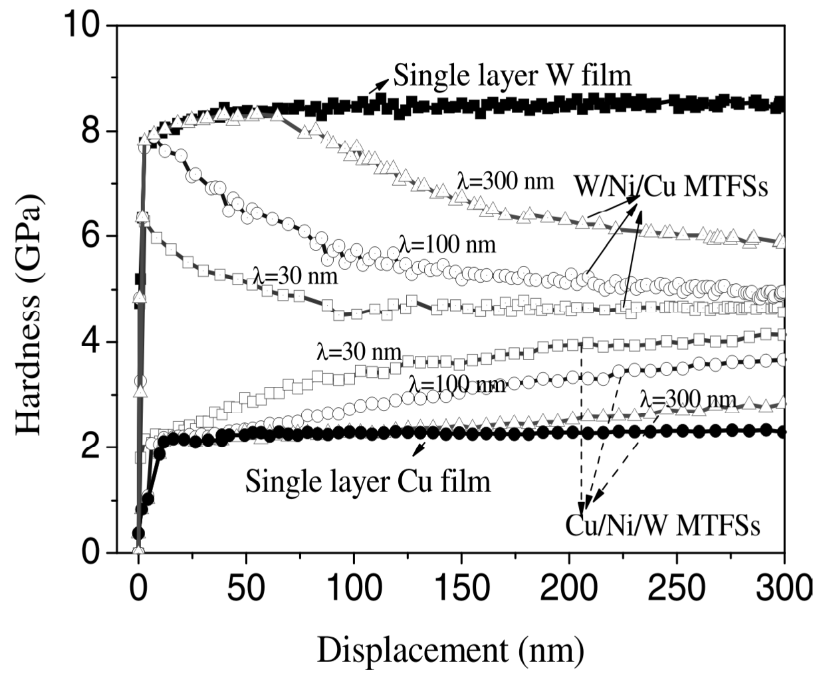

Figure 10: Simulated Variation of Hardness with Indentation Depth

3.4. Pile-up Behavior

Fig. 11a is a schematic of indentation pile-up after complete unloading, where h_p is the pile-up depth, h_r is the residual indentation depth and a_r is the residual indentation impression radius. The pile-up ratio is normally expressed as h_p/h_r. Fig. 11b shows the evaluated variation of pile-up ratio (h_p/h_r) with the individual thickness λ for the Cu/Ni/W and W/Ni/Cu MTFSs. The results for the single layered films are also included. It can be seen that the pile-up ratio in the Cu/Ni/W film clearly increases with the individual layer thickness λ and is higher than the single layered films but opposite trend is observed in the W/Ni/Cu film. A similar pile-up behavior was observed in the plastically graded materials [15]. Figs. 12~14 show the contours of equivalent plastic strain underneath the indenter for the single layered films, Cu/Ni/W and W/Ni/Cu MTFSs, corresponding to an indentation depth of 300 nm before unloading. For the single layered films, the highest equivalent plastic strain is observed in the Cu film. With increasing the indentation depth, the area occupied by the high equivalent plastic strain (plastic zone) extends gradually in the lateral and vertical directions. The length of the plastic zone along the lateral direction in the Cu film is greater than that in the Ni and W films. For the Cu/Ni/W multi-layered films, as shown in Fig. 13, the length of the plastic zone along the lateral direction increases with the individual layer thickness λ. On the other hand, larger plastic zone in the lateral direction is observed in the W/Ni/Cu film with smaller individual layer thickness λ. Therefore, it is interesting to note that the pile-up ratio is proportional to the evolution of plastic zone in the lateral direction. It is believed that the difference in yield strength in the individual layers (plastic mismatch) and the geometrical constraint by the interfaces will contribute to the development of the plastic zone in these MTFSs. Further work is certainly required.

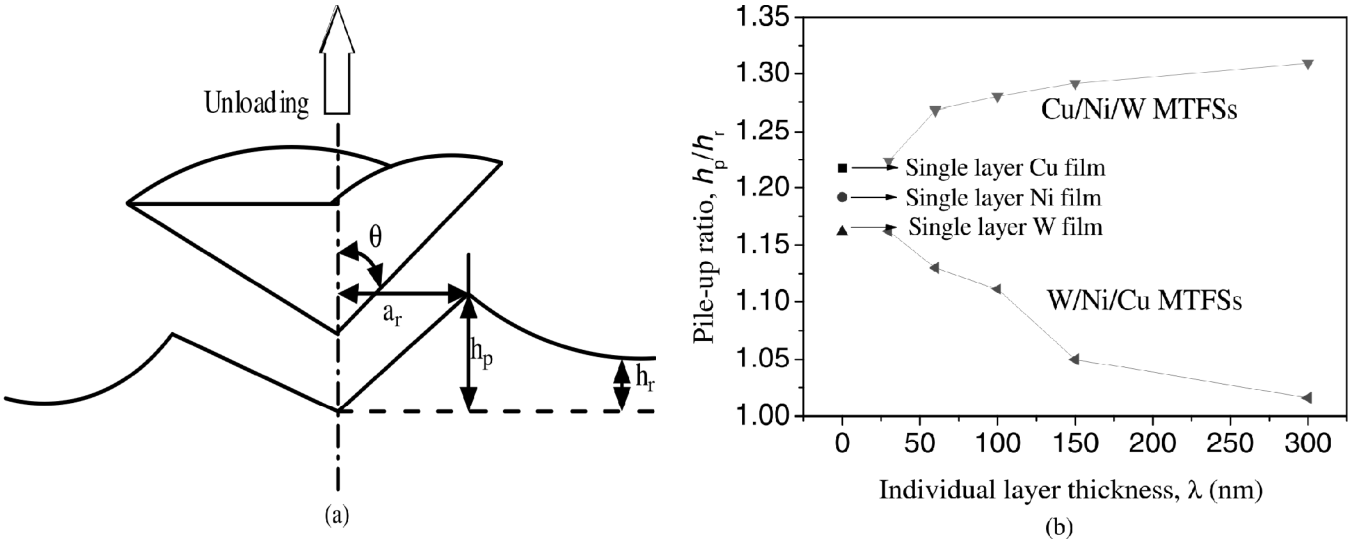

Figure 11: (a) Schematic of Pile-up around an Indenter after Complete Unloading and (b) Simulated Pile-up Ratio versus the Individual Layer Thickness λ

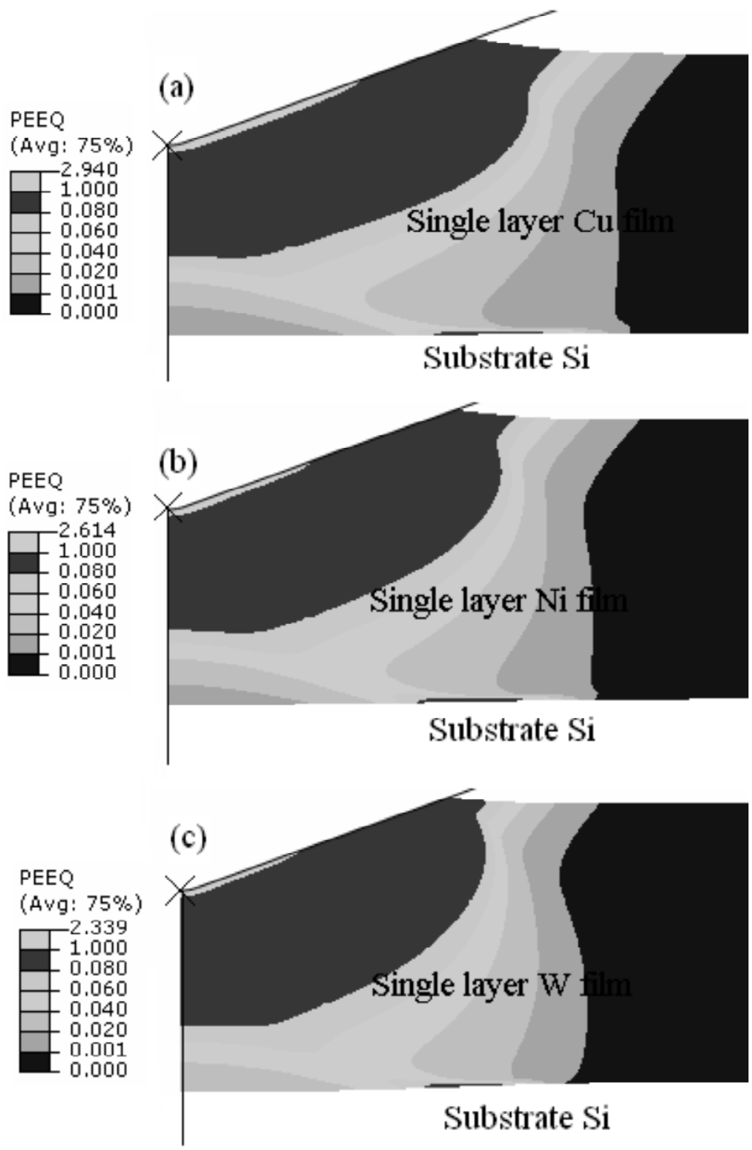

Figure 12: Contours of Equivalent Plastic Strain in Single Layered (a) Cu, (b) Ni and (c) W Films

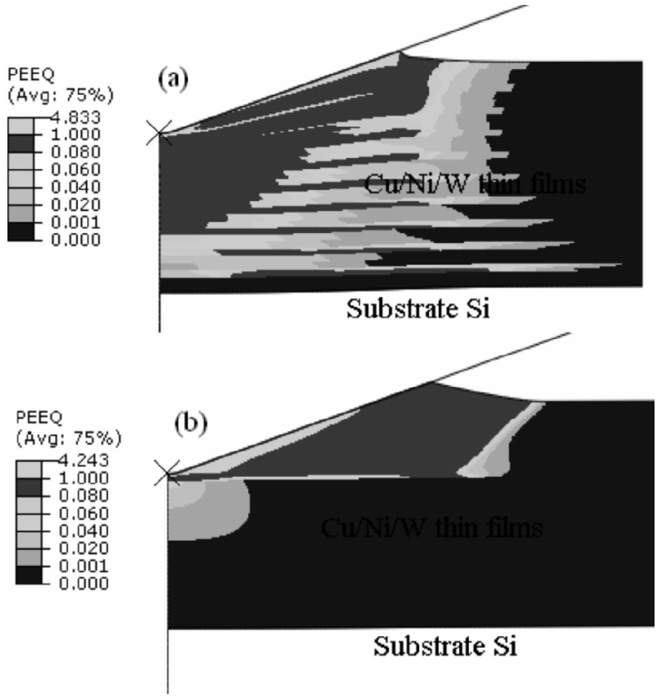

Figure 13: Contours of Equivalent Plastic Strain in the Cu/Ni/W MTFSs with Various λ: (a) 30 nm and (b) 300 nm

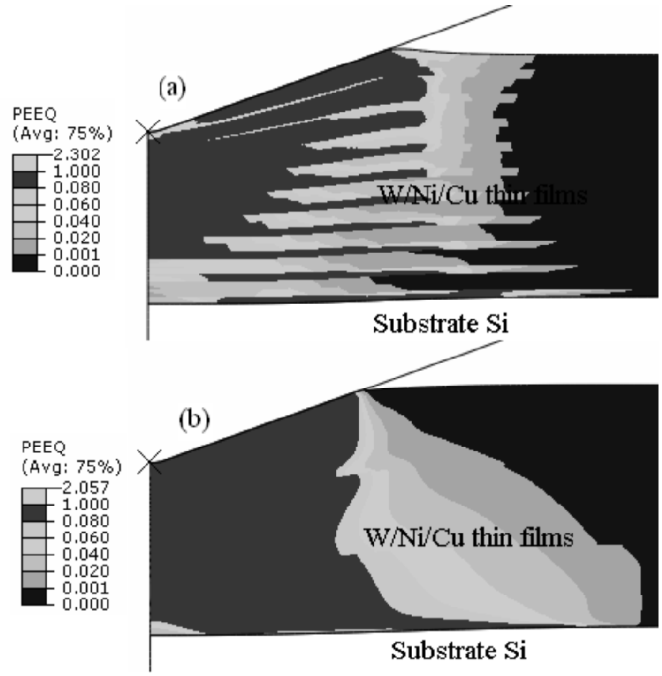

Figure 14: Contours of Equivalent Plastic Strain in the Cu/Ni/W MTFSs with various λ: (a) 30 nm and (b) 300 nm

4. CONCLUSION

Based on the finite element analysis of the nanoindentation behavior of the MTFSs, several conclusions can be drawn, which are as follows:

The indentation depth required to drive the plastic zone to the interface with the adjacent layer can be considered as a critical penetration depth above which the indentation response is controlled by all constituting layers in a MTFS rather than the top layer.

For the Cu/Ni/W MTFSs (soft layer on the top), the thinner the individual layer thickness, the smaller the critical penetration depth and the higher the hardness can be observed in our simulations. If the stacking sequence is changed in a MTFS, such as W/Ni/Cu (hard layer on the top), the numerical simulation indicates an opposite effect of the individual layer thickness on hardness and the critical indentation depth.

The pile-up ratio around the indenter was investigated numerically in the Cu/Ni/W MTFSs. Both individual layer thickness and the stacking sequence will affect the pile-up. It was found in the numerical simulation that the pile-up ratio is proportional to the evolution of plastic zone in the lateral direction.

Acknowledgement

C. Yan acknowledges the support of a DEST China-Australia fund and two ARC Discovery Projects. The first author would appreciate the National Science Foundation of China (10902048), the Foundation of Jiangxi Educational Committee (GJJ08229) and the Natural Science Foundation of Jiangxi Province of China (2008GZW0010). QUT's High Performance Computing & Research Support (HPC) has kindly provided access to its facilities and ABAQUS 6.7.

References

[1] Tan, X. H. and Shen, Y. L., "Modeling Analysis of the Indentation-derived Yield Properties of Metallic Multilayered Composites," *Sci. Tech.*, **65**, 1639-1646, (2005).

[2] Harry, E., Ignat, M., Rouzaud, A. and Juliet, P., "Cracking Investigation of W and W(C) Films Deposited by Physical Vapor Deposition on Steel Substrates," *Surf. Coat. Technol.*, **111**, 177–183, (1999).

[3] Wen, S. P., Zong, R. L., Zeng, F., Gao Y. and Pan, F., "Evaluating Modulus and Hardness Enhancement in Evaporated Cu/W Multilayers," *Acta Mater.*, **55**, 345–351, (2007).

[4] Gouldstone, A., Chollacoop, N., Dao, M., Li, J., Minor, A. M. and Shen, Y. L., “Indentation Across Size Scales and Disciplines: Recent Developments in Experimentation and Modelling,” *Acta Mater.*, **55**, 4015-4039, (2007).

[5] Bull, S. J., “Modelling the Hardness Response of Bulk Materials, Single and Multilayer Coatings,” *Thin Solid Films*, 398-399, 291-298, (2001).

[6] Barshilia, H. C. and Rajam, K. S., “Characterization of Cu/Ni multilayer Coatings by Nanoindentation and Atomic Force Microscopy,” *Surf. Coat. Technol.*, **155**, 195-202, (2002).

[7] Martinez, E., Romero, J., Lousa, A. and Esteve, J., “Nanoindentation Stress–strain Curves as a Method for Thin-film Complete Mechanical Characterization: Application to Nanometric CrN/Cr Multilayer Coatings,” *Appl. Phys.* A, **77**, 419-426, (2003).

[8] Panich, N. and Sun Y., “Effect of Penetration Depth on Indentation Response of Soft Coatings on Hard Substrates: A Finite Element Analysis,” *Surf. Coat. Technol.*, **182**, 342-350, (2004).

[9] Tsui, T. Y. and Pharr, G. M., “Substrate Effects on Nanoindentation Mechanical Property Measurement of Soft Films on Hard Substrates,” *J. Mater. Res.*, **14**, 292-301, (1999).

[10] Lebouvier, D., Gilormini, P. and Felder, E., “A Kinematic Solution for Plane-strain Indentation of a Bi-layer**,”** *J. Phys. D: Appl. Phys.*, **18**, 199-210, (1985).

[11] Sun, Y., Bell, T. and Zheng, S., “Finite Element Analysis of the Critical Ratio of Coating Thickness to Indentation Depth for Coating Property Measurements by Nanoindentation,” *Thin Solid Films*, **258**, 198-204, (1995).

[12] Bolshakov, A. and Pharr, G. M., “Influences of Pileup on the Measurement of Mechanical Properties by Load and Depth Sensing Indentation Techniques,” *J. Mater. Res.*, **13**, 1049-1058, (1998).

[13] Cheng, Y. T. and Cheng, C. M., “Scaling, Dimensional Analysis, and Indentation Measurements,” *Mater. Sci. Eng. R*, **44**, 91-149, (2004).

[14] Wang, L. and Rokhlin, S. I., “Universal Scaling Functions for Continuous Stiffness Nanoindentation with Sharp Indenters,” *Int. J. Solids. Struct.*, **42**, 3807-3832, (2005).

[15] Choi, I. S. and Suresh, M. D., “Mechanics of Indentation of Plastically Graded Materials—I: Analysis,” *J. Mech. Phys. Solids*, **56**, 157-171, (2008).

[16] Huang, X. and Pelegri, A., “Mechanical Characterization of Thin Film Materials with Nanoindentation Measurements and FE Analysis,” *J. Compos. Mater.*, **40**, 1393-1406, (2006).

[17] Dassault Systems Simulia Corp, “ABAQUS Theory Manual, Version 6.7,” Providence, (2007).

[18] Brandstetter, S., Zhang, K., Escuadro, A., Weertman, J. R. and Swygenhoven, H. V., “Grain Coarsening During Compression of Bulk Nanocrystalline Nickel and Copper,” *Scripta Mater.*, **58**, 61-64, (2008).

[19] Qasmi, M., Delobelle, P., Richard, F. and Bosseboeuf, A., “Effect of the Residual Stress on the Determination Through Nanoindentation Technique of the Young’s Modulus of W thin Film Deposit on SiO2/Si Substrate,” *Surf. Coat. Technol.*, **200**, 4185–4194, (2006).

[20] Hemker, K. J. and Jr Sharpe, W. N., “Microscale Characterization of Mechanical Properties,” *Annu. Rev. Mater. Res.*, **37**, 93-126, (2007).

[21] Chawla, N., Singh, D. R. P., Shen, Y. L., Tang, G. and Chawla, K. K., “Indentation Mechanics and Fracture Behaviour of Metal/ceramic Nanolaminate Composites,” *J. Mater. Sci.*, **43**, 4383-4390, (2008).